In situ construction oxygen vacancy-rich and fluorine doped carbon coated $Ca_2Fe_2O_5$ for improved lithium storage performance

Piao Zhu, [a] Gang Yang, [a] Xiujuan Sun, *[a] Qiuhan Cao, [a] Yongjie Zhao, [a] Rui Ding, [a] Enhui Liu*[a]and Ping Gao[a]

[a] P.Zhu, G.Yang, X.J.Sun, Q.H.Cao, Y.J.Zhao, R.Ding, E.H.Liu, P.Gao
Key Laboratory of Environmentally Friendly Chemistry and Applications of Ministry of Education, College of Chemistry, Xiangtan University, Hunan 411105, P.R. China.
E-mail: sunxj594@xtu.edu.cn; liuenhui@xtu.edu.cn

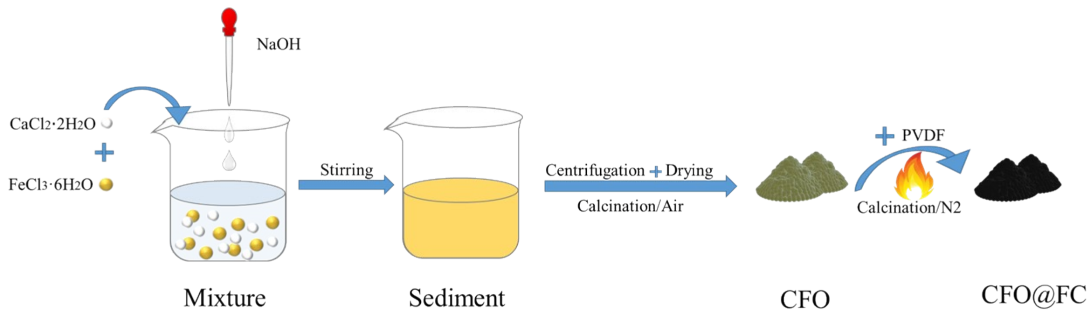

Figure S1. Preparation scheme for CFO@FC.

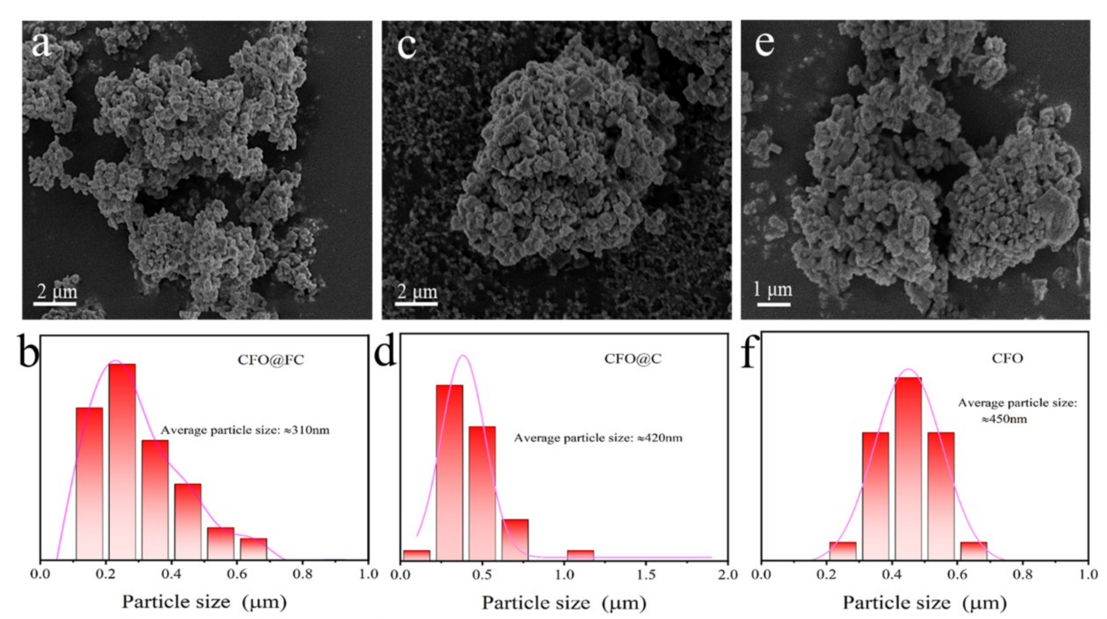

Figure S2. The statistical images of the CFO@FC, CFO@C and CFO samples (a), (c) (e) and their respective corresponding particle size distributions (b), (d) (f).

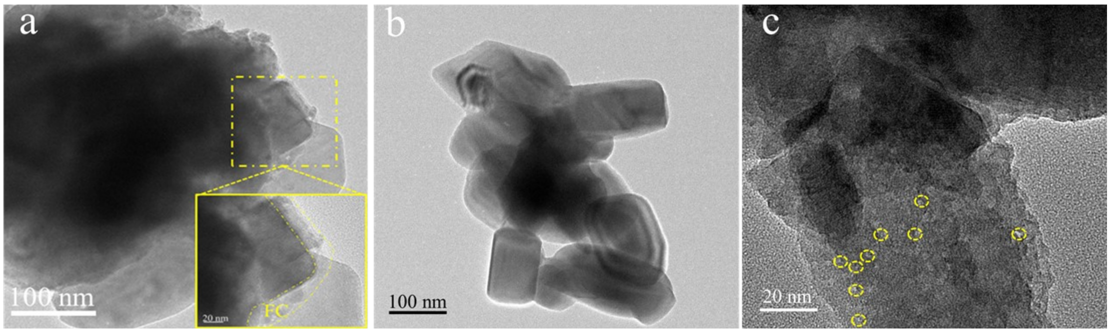

Figure S3. The TEM image of CFO@FC sample(a) (c) and CFO sample(b).

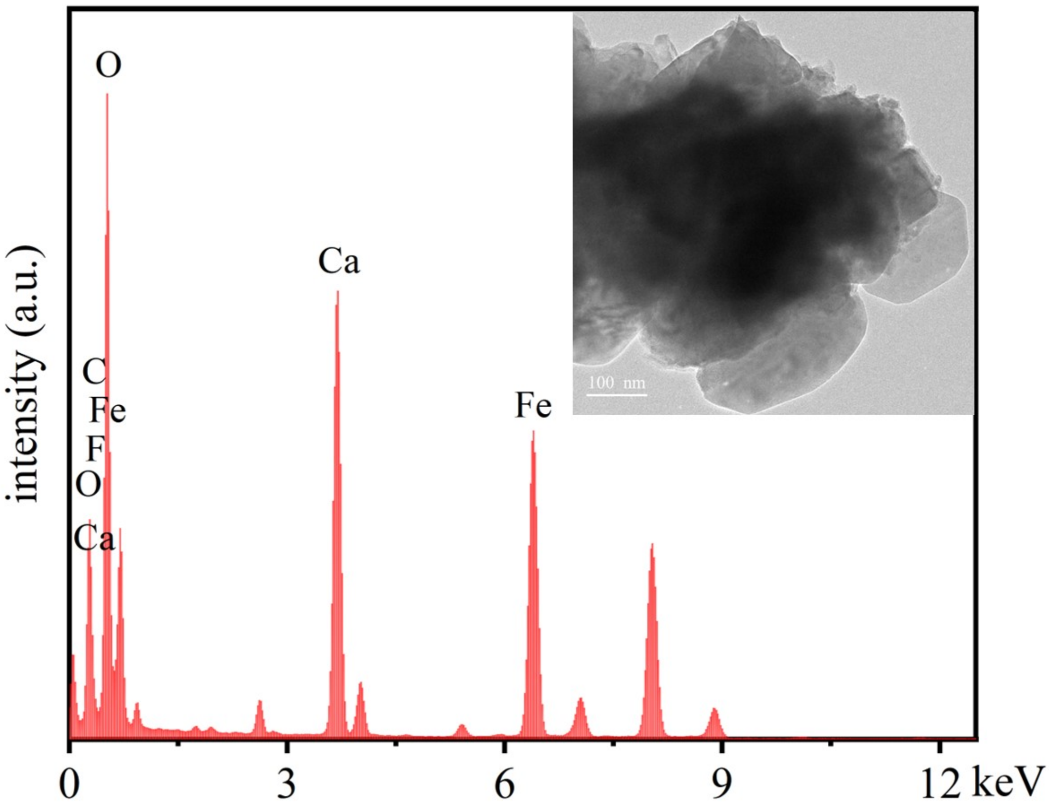

Figure S4. The EDS (inset is the TEM figure) image of the CFO@FC sample.

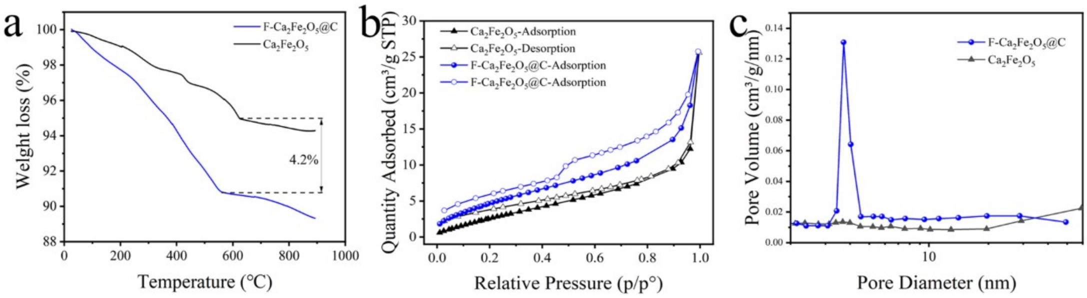

Figure S5. Thermogravimetric analysis of CFO@FC(a); nitrogen adsorption/desorption isotherms (b), pore volumes (c) of CFO@FC and CFO.

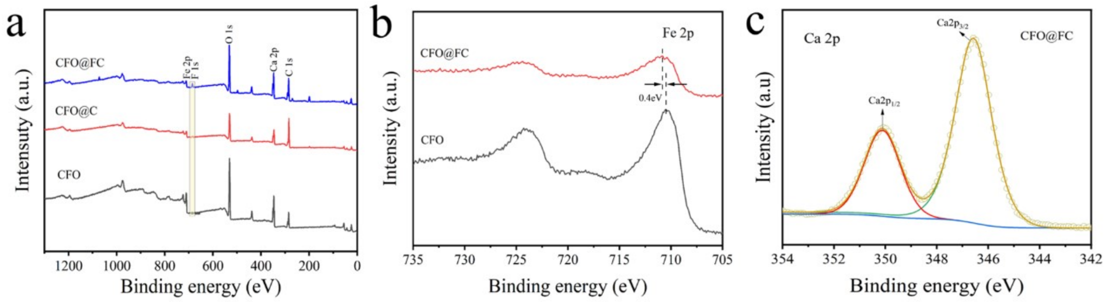

Figure S6. The XPS survey spectrum of CFO@FC, CFO@C, and CFO samples(a); the comparison of high-resolution XPS spectra of Fe 2p of CFO@FC and CFO (b); Ca 2p (c) of the CFO@FC samples.

Table. S1. The atomic percent of the samples derived from the quantitative analysis of the XPS spectra.

Atomic (%)	Ca2p	Fe2p	O1s	C1s	F1s	O(1s)/[Ca(2p) +Fe(2p)]
CFO@FC	10.71	9.44	28.1	48.77	2.98	1.39
CFO@C	11.67	10.71	35.51	42.11	0	1.59
CFO	12.35	11.54	49.63	26.48	0	2.08

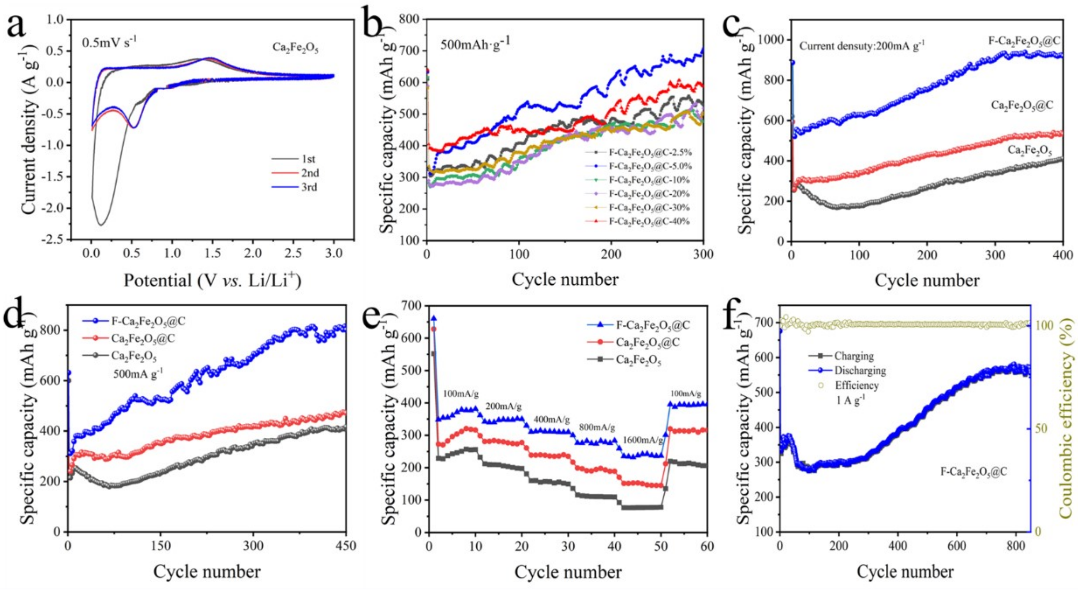

Figure S7. The cyclic voltammetry of CFO at 0.5 mV·s^{-1} (a), cycle performance of CFO@FC with different amounts of fluorine doping (b), cycle performance of CFO@FC, CFO@C and CFO electrodes at 200 mA g^{-1} (c), cycle performance of CFO@FC, CFO@C and CFO electrodes at 500 mA g^{-1} (d), rate performance from 100 to 1600m A g^{-1} of CFO@FC, CFO@C and CFO electrodes (e), cycle performance of CFO@FC at 1 A g^{-1}(f).

Table S2. Comparison of CFO@FC nanoparticles (this work) with various Iron-based oxides as anodes for LIBs.

material	synthetic method	Li-storage performance (specific capacity (mAh g^{-1}) @current density (mA g^{-1}) @cycles	ref
$Ca_2Fe_2O_5$	solid-state reaction	183@60@50	1
$Ca_2Co_2O_5$	solid-state reaction	380@60@50	1
$Ca_2Fe_2O_5$	electrospinning	530@50@100	2
$Ca_2Fe_2O_5$ nanoparticles	combustion method	240@75@50	3
$Ca_2Fe_2O_5$ nanofibers	electrospinning	622@50@75; 485 @200@250	3
$Sr_2Fe_2O_{6-\delta}$	solid-state synthesis	393@25@50	4
Fe_2O_3 powder	heat treatment	500@50@50	5
orthorhombic $CaFe_2O_4$ microrod	co-precipitation	400@500@100	6
porous $CaFe_2O_4$	combustion method	551@200@150	7
Nanorod-shaped $NaFeSnO_4$	solid-state reaction	179@10@200	8
$CaFe_2O_4$	solid-state reaction	200@60@50	9
$Li_{0.5}Ca_{0.5}(Fe_{1.5}Sn_{0.5})O_4$	solid-state reaction	405@60@50	9
$MgFe_2O_4$ nanoparticles	Sol-gel method	293@90@50	10
Fe_2O_3	template-assisted method	190@100@150	11
CFO@FC nanoparticles	heat treatment	927@200@400; 815@500@450; 572@1000@820;	This work

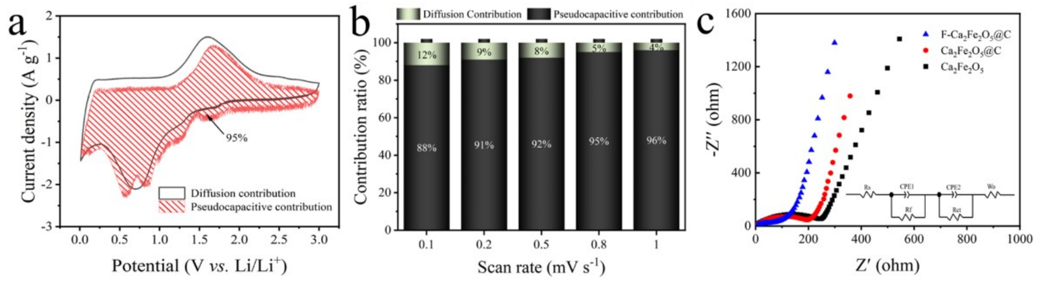

Figure S8. The capacitive and diffusion contribution at a scan rate of 5 mV·s−1(a), the normalized ratio values of pseudocapacitive and diffusion contribution at 0.1–1.0 mV s−1 of CFO@FC (b), the Nyquist plots in the frequency range of 100 kHz to 0.01 Hz, the corresponding equivalent circuits (the insert image) of CFO@FC, CFO@C and CFO electrode(c).

Table S3. Various parameters were obtained from the Nyquist plot fitting of the CFO@FC, CFO@C and CFO electrodes.

Electrode	Rs(Ω)	Rf(Ω)	Rct(Ω)
CFO@FC	6.00	7.53	26.18
CFO@C	3.12	12.31	141.50
CFO	2.66	28.16	216.70

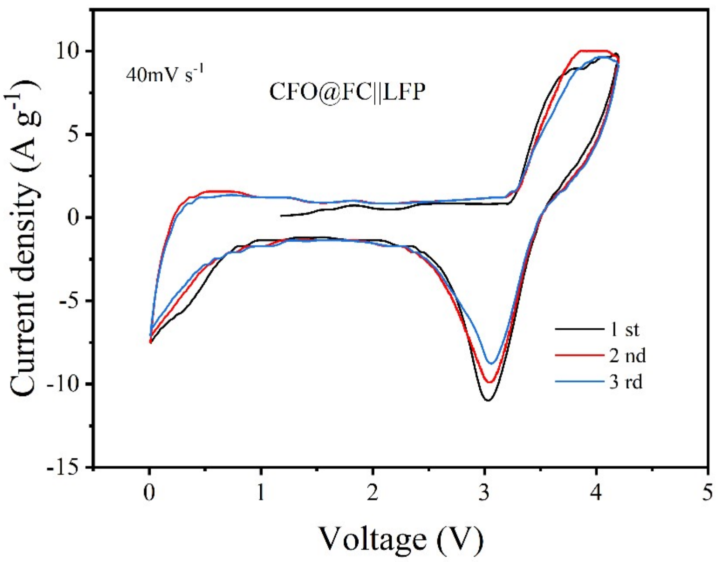

Figure S9. CV curve of CFO@FC at 40 mV s^{-1}.

References

1. N. Sharma, K. M. Shaju, G. V. Subba Rao and B. V. R. Chowdari, *Electrochim Acta*, 2004, **49**, 1035-1043.
2. S. K. Sundriyal and Y. Sharma, *Appl Surf Sci*, 2021, **560**.
3. S. K. Sundriyal and Y. Sharma, *Acs Appl Energ Mater*, 2020, **3**, 6360-6373.
4. R. K. Hona, A. K. Thapa and F. Ramezanipour, *Chemistryselect*, 2020, **5**, 5706-5711.
5. J. E. Hong, R. G. Oh and K. S. Ryu, *Environ Sci Pollut R*, 2016, **23**, 14656-14662.
6. K. Zhang, W. Hong, P. Gao, R. Ding and E. Liu, *Int J Hydrogen Energ*, 2020, **45**, 22160-22165.
7. N. Shaji, P. Santhoshkumar, M. Nanthagopal, C. Senthil and C. W. Lee, *Appl Surf Sci*, 2019, **491**, 757-764.
8. D. S. Bhange, D. A. Anang, G. Ali, J.-H. Park, J.-Y. Kim, J.-H. Bae, W. Y. Yoon, K. Y. Chung and K.-W. Nam, *Electrochem Commun*, 2020, **121**.
9. N. Sharma, K. M. Shaju, G. V. Subba Rao and B. V. R. Chowdari, *J Power Sources*, 2003, **124**, 204-212.
10. Y. Pan, Y. Zhang, X. Wei, C. Yuan, J. Yin, D. Cao and G. Wang, *Electrochim Acta*, 2013, **109**, 89-94.
11. S. Li, Y. Zhang and J. Huang, *J Alloy Compd*, 2019, **783**, 793-800.